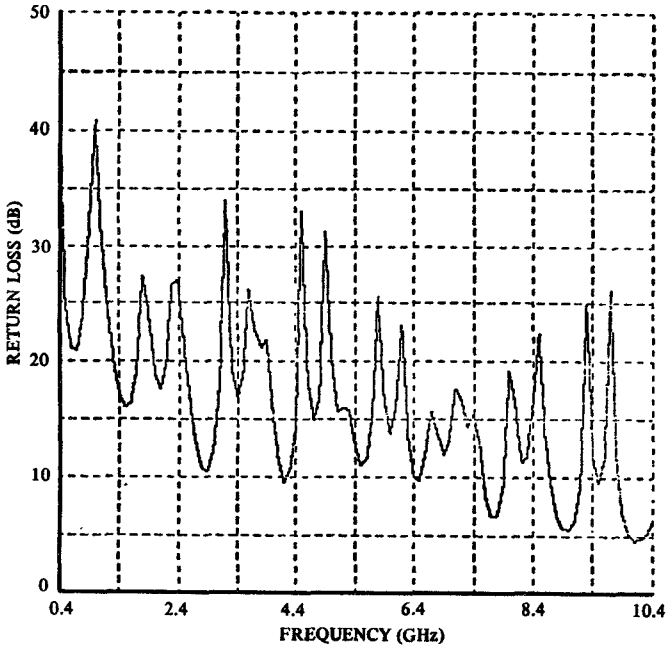

Fig. 8. Return loss of magic tee.

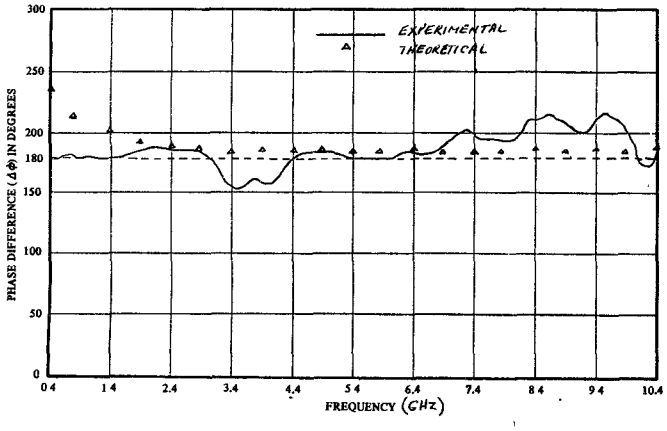

Fig. 9. Phase performance of tapered asymmetric magic tee.

top ground plane, undesirable ripples are induced in the coupling. Also, each coupler section and reference line was made on individual substrates and metal walls separated the substrates in order to reduce spurious modes.

The magic tee circuit designed for a low-frequency cutoff of 1 GHz is shown in Fig. 5 with the top ground plane removed. The actual characteristics of this device are shown in Figs. 6–9. Fig. 6 compares power at the two equal-power output ports. The average power deviation is less than 0.5 dB over the 1–9-GHz frequency band. Fig. 7 shows the isolation and Fig. 8 shows the return loss. Fig. 9 depicts the measured and the computed phase difference between the output ports of the magic tee.

CONCLUSION

This work has demonstrated the feasibility of designing a decade-wide magic tee, using microstrip and a top ground plane. The coupling factor $k(z)$, which changes continuously along the length of the coupler, was calculated for this device using the coupling coefficient prepared by Arndt for equal-ripple high-pass directional couplers. The line and gap widths were determined by using the computer subroutine of Smith. The coupled sections and the reference lines were separated by metal walls in order to reduce the standing-wave modes in the box.

ACKNOWLEDGMENT

The authors wish to thank F. A. Pizzarello and D. E. Stiegler for their efforts in fabricating the circuits.

REFERENCES

[1] F. C. De Ronde, "A new class of microstrip directional couplers," in *IEEE G-MTT Symp. Dig.*, May 1970, pp. 184–189.
[2] E. Carpenter, "The virtue of mixing tandem and cascade coupler connections," in *IEEE G-MTT Symp. Dig*, May 1971, pp. 8–9.
[3] F. Arndt, "Tables for asymmetric Chebyshev high-pass TEM-mode directional couplers," *IEEE Trans. Microwave Theory Tech.*, vol. MTT-18, pp. 633–638, Sept. 1970.
[4] C. P. Tresselt, "Design and computed theoretical performance of three classes of equal-ripple nonuniform line couplers," *IEEE Trans. Microwave Theory Tech.*, vol. MTT-17, pp. 218–230, Apr. 1969.
[5] R. H. Duhamel and M. E. Armstrong, "The tapered-line magic-T: A wide-band monopulse antenna," in *Abstracts of the 15th Annu. Symp. USAF Antenna Research and Development Program* (Monticello, Ill.), Oct. 12–14, 1965.
[6] H. J. Hindin and A. Rosenzweig, "3-dB couplers constructed from two tandem connected 8.34-dB asymmetric couplers," *IEEE Trans. Microwave Theory Tech.* (Corresp.), vol. MTT-16, pp. 125–126, Feb. 1968.
[7] E. G. Cristal and S. Frankel, "Design of hairpin-line and hybrid hairpin-parallel-coupled-line filters," in *IEEE G-MTT Symp. Dig.*, May 1971, pp. 12–13.
[8] J. I. Smith, "The even- and odd-mode capacitnace parameters for coupled lines in suspended substrate," *IEEE Trans Microwave Theory Tech.*, vol. MTT-19, pp. 424–431, May 1971.

Evaluation of the Equivalent Circuit Parameters of Microstrip Discontinuities Through Perturbation of a Resonant Ring

WOLFGANG J. R. HOEFER, MEMBER, IEEE, AND
ASOKNATH CHATTOPADHYAY, STUDENT MEMBER, IEEE

***Abstract*—A resonant technique for evaluating the equivalent circuit of reciprocal microstrip discontinuities is described. The complex Z parameters of a discontinuity are related to the change in resonant frequencies and Q factors of a microstrip ring it perturbs. As an example, measurements made on inductive posts are presented and compared with theoretical values.**

I. INTRODUCTION

The main difficulty in measuring the circuit parameters of microstrip discontinuities resides in the elimination of systematic errors introduced by coaxial–to–microstrip transitions. This problem can be avoided by testing discontinuities in a resonant microstrip ring which may be coupled very loosely to the test equipment.

Stephenson and Easter [1] and Douville and James [2] have demonstrated the resonant technique as applied to the characterization of rectangular bends. Groll and Weidmann [3] have evaluated impedance steps in a resonant ring.

The present short paper gives a comprehensive general analysis of a microstrip ring containing a reciprocal discontinuity. First it is shown how the Z parameters of a discontinuity are related to the change in resonant frequencies and Q factors of a microstrip ring it perturbs. Then the measurement technique is described, the accuracy of the method is discussed, and some measurements made on inductive metallic posts are presented.

Manuscript received April 14, 1975; revised August 25, 1975. This work was supported in part by the National Research Council of Canada under Grant A 7620, and in part by the Communications Research Centre, Ottawa, Ont., Canada.

The authors are with the Department of Electrical Engineering, University of Ottawa, Ottawa, Ont., Canada.

II. ANALYSIS OF THE RESONANT RING CONTAINING A RECIPROCAL DISCONTINUITY

In the present analysis, a microstrip ring is a microstrip transmission line which is closed in itself. All radii of curvature are large with respect to the strip width so that the fields have practically the same configuration as in a straight line of identical cross section.

Such a structure resonates if its electrical length is an integral multiple of the guided wavelength. When a discontinuity is introduced into the ring, each resonance degenerates into two distinct modes. This splitting is conveniently interpreted in terms of even and odd excitation of the discontinuity. The even case corresponds to the incidence of two waves of equal magnitude and phase upon the discontinuity, while in the odd case, waves of equal magnitude but opposite phase are incident from both sides. Either mode of resonance can be suppressed by an appropriate choice of the point of excitation along the ring.

A. Symmetrical Discontinuities

Symmetrical discontinuities can be represented by a symmetrical T or π section in a single reference plane. This plane of electrical symmetry will henceforth be called the $z = 0$ plane.

Fig. 1 shows the equivalent T circuit of a symmetrical discontinuity. For convenience, the circuit is divided into two identical half-sections of zero electrical length. The elements are expressed in terms of Z parameters. If this circuit is excited in the even mode, no current crosses the $z = 0$ plane. Therefore the input impedance of each half-section is not altered if the circuit is bisected in this plane [Fig. 1(b)]. The normalized even input impedance at either port is thus $Z_{ie} = Z_{11} + Z_{12}$.

The normalized odd input impedance, in turn, is $Z_{io} = Z_{11} - Z_{12}$ and represents the impedance of a half-section which is short circuited in the $z = 0$ plane [Fig. 1(c)].

1) *Lossless Symmetrical Discontinuities:* If the discontinuity is lossless, only the resonance frequencies of the perturbed ring are affected since the even and odd impedances are purely reactive. These impedances may be thought of as input impedances of fictitious transmission-line sections which are open (even case) or short circuited (odd case) at the other end [Fig. 2(a) and (b)].

The artificial increase of the electrical length of the ring resulting in the decrease of its resonance frequencies, is related to the normalized even and odd input impedances by the following expressions:

$$Z_{ie} = Z_{11} + Z_{12} = -j \cot k l_e \quad \text{(even case)} \tag{1}$$

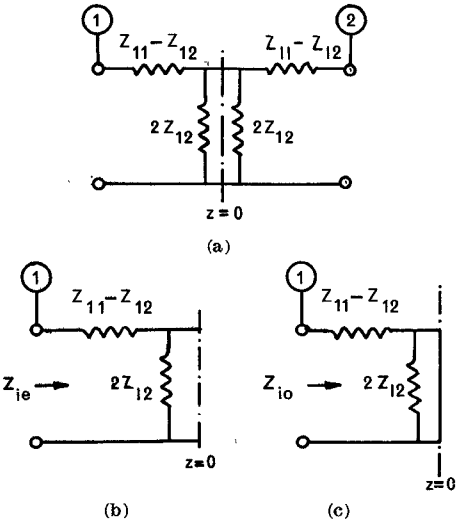

Fig. 1. (a) Equivalent circuit of a symmetrical discontinuity. (b) One half of the equivalent circuit for even excitation. $Z_{ie} = Z_{11} + Z_{12}$. (c) One half of the equivalent circuit for odd excitation. $Z_{io} = Z_{11} + Z_{12}$.

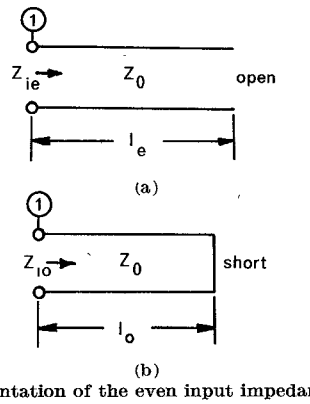

Fig. 2. (a) Representation of the even input impedance Z_{ie} in plane ① by a fictitious open-circuited line (lossless discontinuity). (b) Representation of the odd input impedance Z_{io} in plane ① by a fictitious short-circuited line (lossless discontinuity).

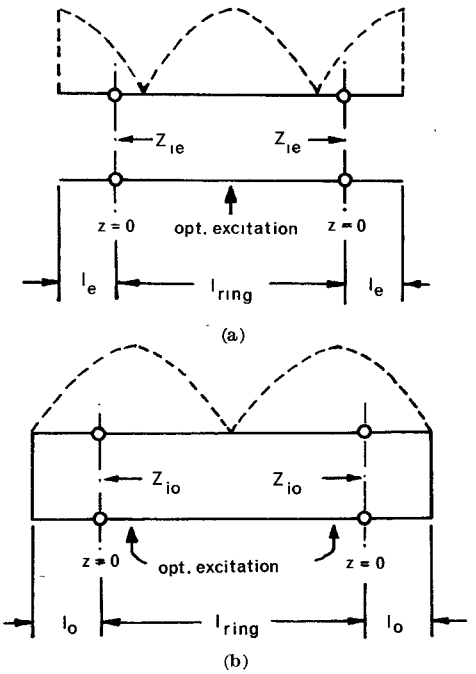

Fig. 3. (a) Standing-wave pattern on the ring for even excitation of the discontinuity ($n = 1$). (b) Standing-wave pattern on the ring for odd excitation of the discontinuity ($n = 1$).

$$Z_{io} = Z_{11} - Z_{12} = j \tan k l_o \quad \text{(odd case)} \tag{2}$$

where $k = 2\pi/\lambda_t$ is the propagation constant of the quasi-TEM mode.

Fig. 3(a) and (b) shows the standing-wave pattern on the ring resonating in the fundamental mode. For convenient presentation, the ring is cut open at $z = 0$ and straightened out. The fictitious lines representing Z_{ie} and Z_{io} have been added on either side.

Since at resonance the total electrical length of the resonator (including the discontinuity) is $n \cdot \lambda_t$, where n is the harmonic number, the resonance conditions are, in the even case,

$$l_{ring} + 2l_e = n\lambda_{te} \tag{3}$$

and in the odd case,

$$l_{ring} + 2l_o = n\lambda_{to} \tag{4}$$

where l_{ring} is the physical length of the ring along the mean circumference, and λ_{te} and λ_{to} are the guided wavelengths corresponding to the even and odd resonance frequency, respectively. Since l_{ring} is known and λ_t can be obtained from measurements, l_e and l_o

are determined from (3) and (4). When introduced into (1) and (2), respectively, they yield

$$Z_{11} + Z_{12} = -j \cot \left[\tfrac{1}{2}k\,(n\lambda_{te} - l_{\text{ring}})\right] = j \cot\left(\pi \frac{l_{\text{ring}}}{\lambda_{te}}\right) \quad (5)$$

$$Z_{11} - Z_{12} = j \tan \left[\tfrac{1}{2}k\,(n\lambda_{to} - l_{\text{ring}})\right] = -j \tan\left(\pi \frac{l_{\text{ring}}}{\lambda_{to}}\right). \quad (6)$$

Since one measures resonance frequencies rather than wavelengths, it is more convenient to express λ_{te} and λ_{to} as follows:

$$\lambda_{te} = c/(f_{re}\left[\epsilon_{\text{eff}}(f_{re})\right]^{1/2}) \quad (7)$$

$$\lambda_{to} = c/(f_{ro}\left[\epsilon_{\text{eff}}(f_{ro})\right]^{1/2}) \quad (8)$$

and to introduce these expressions into (5) and (6), respectively. Thus

$$Z_{ie} = Z_{11} + Z_{12} = j \cot \frac{\pi l_{\text{ring}}\left[\epsilon_{\text{eff}}(f_{re})\right]^{1/2} f_{re}}{c} \quad (9)$$

$$Z_{io} = Z_{11} - Z_{12} = -j \tan \frac{\pi l_{\text{ring}}\left[\epsilon_{\text{eff}}(f_{ro})\right]^{1/2} f_{ro}}{c} \quad (10)$$

where $\epsilon_{\text{eff}}(f)$ is the dispersive effective dielectric constant of the ring, c is the speed of light, and f_{re} and f_{ro} are the even and odd resonance frequencies of the perturbed ring. These expressions form the basis for the measurement technique described in the following.

2) *Lossy Symmetrical Discontinuities:* Dissipation and radiation losses render the Z parameters of discontinuities complex. The complex even and odd input impedances of the equivalent circuit can be represented by sections of transmission lines terminated in a pure resistance [Fig. 4(a) and (b)].

The terminating resistance must be larger than Z_0 in the even case (voltage maximum at $z = 0$) and smaller than Z_0 in the odd case (voltage minimum at $z = 0$). Note that for the lossless case, R tends towards ∞ while r becomes zero.

The lengths and terminations of the fictitious lines are such that

$$Z_{ie} = Z_{11} + Z_{12} = \frac{\dfrac{R}{Z_0} + j \tan kl_e}{1 + j\dfrac{R}{Z_0}\tan kl_e} = \frac{\dfrac{R}{Z_0} - j \tan\left(\pi \dfrac{l_{\text{ring}}}{\lambda_{te}}\right)}{1 - j\dfrac{R}{Z_0}\tan\left(\pi \dfrac{l_{\text{ring}}}{\lambda_{te}}\right)} \quad (11)$$

$$Z_{io} = Z_{11} - Z_{12} = \frac{\dfrac{r}{Z_0} + j \tan kl_o}{1 + j\dfrac{r}{Z_0}\tan kl_o} = \frac{\dfrac{r}{Z_0} - j \tan\left(\pi \dfrac{l_{\text{ring}}}{\lambda_{to}}\right)}{1 - j\dfrac{r}{Z_0}\tan\left(\pi \dfrac{l_{\text{ring}}}{\lambda_{to}}\right)}. \quad (12)$$

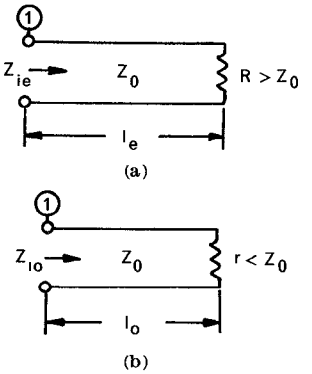

Fig. 4. (a) Representation of the even input impedance Z_{ie} of a lossy discontinuity in plane ① by a fictitious line terminated in $R > Z_0$. (b) Representation of the odd input impedance Z_{io} of a lossy discontinuity in plane ① by a fictitious line terminated in $r < Z_0$.

The wavelengths λ_{te} and λ_{to} satisfy (7) and (8), respectively, and are determined as in the lossless case. R and r affect the Q factor of the ring. Let Q_l be the unloaded Q of the ring, while Q_{2e} and Q_{2o} are the loaded Q factors of the ring for even and odd excitation of the discontinuity, respectively. Then

$$\frac{R}{Z_0} = \frac{2}{\pi n}\frac{Q_l Q_{2e}}{Q_l - Q_{2e}} \quad (13)$$

$$\frac{r}{Z_0} = \frac{\pi n}{2}\frac{Q_l - Q_{2o}}{Q_l Q_{2o}} \quad (14)$$

where n is the harmonic number.

The circuit parameters Z_{11} and Z_{12} are determined from R, λ_{te}, r, and λ_{to} using (11) and (12).

B. Unsymmetrical Discontinuities

1) *Lossless Unsymmetrical Discontinuities:* A lossless unsymmetrical discontinuity can always be transformed into a symmetrical two-port by adding an appropriate length of line l_a to one of its ports. The plane of electrical symmetry $z = 0$ is then situated halfway between the planes with respect to which the two-port is symmetrical. Once the Z parameters in the plane $z = 0$ are known, the impedance in any other plane can be found by simple transformation along the line.

In practice, the $z = 0$ plane is easily determined since it is situated opposite to the point of optimum excitation of the ring at the fundamental even resonance.

2) *Lossy Unsymmetrical Discontinuities:* The concept of symmetrical even and odd excitation can be applied only to those lossy unsymmetrical discontinuities which can be transformed into a symmetrical two-port by adding an appropriate length of line to one of their ports. In terms of S parameters, this condition is fulfilled if

$$|S_{11}| = |S_{22}|.$$

The Z parameters in the plane of electrical symmetry are then calculated using (11) and (12).

III. THE MEASUREMENT TECHNIQUE

The measurement of discontinuity parameters is performed in two steps.

1) The resonant frequencies and unloaded Q factors of the ring are measured before the discontinuity is introduced.

2) The discontinuity is then introduced (either into the same ring or, if this is impractical, into another identical ring), and the even and odd resonant frequencies, together with the corresponding loaded Q factors of the structure, are measured.

The ring should be as uniform as possible since even a small irregularity may introduce effects of the same order as the effects to be measured. The ring is best excited by a capacitive launcher which can be moved along the outer contour of the ring for about one quarter of its circumference to select the optimal point of excitation for each resonance. Coupling should be as light as the sensitivity of the measuring equipment permits. Even then the launcher changes the resonant frequencies slightly. But as long as the measurements on the empty and the perturbed ring are made at the same coupling strength, the effect of the launcher is eliminated since it affects all measurements in the same way.

Resonant frequencies are determined from either reflection or transmission measurements. The former method has the advantage that only one coupling link between ring and peripheral equipment is required. Care must be taken to measure all resonant frequencies with the best possible accuracy since the discontinuity impedance values are very sensitive to frequency variations. This accuracy is limited by the sharpness of the resonance response rather than the performance of available counters for the microwave range.

Changes in temperature alter the resonant frequencies of the ring.

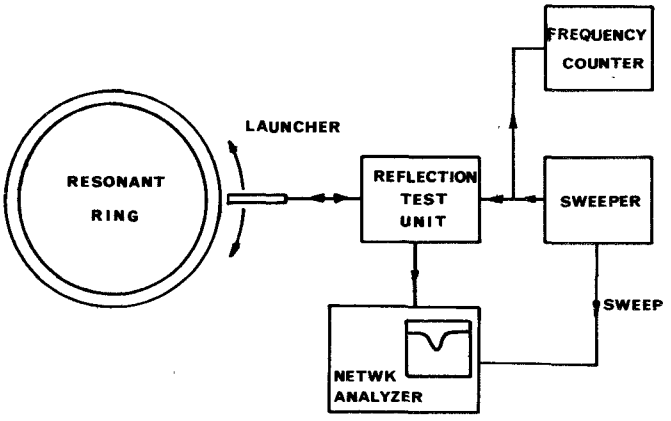

Fig. 5. Arrangement for measuring the resonance frequencies of a microstrip ring.

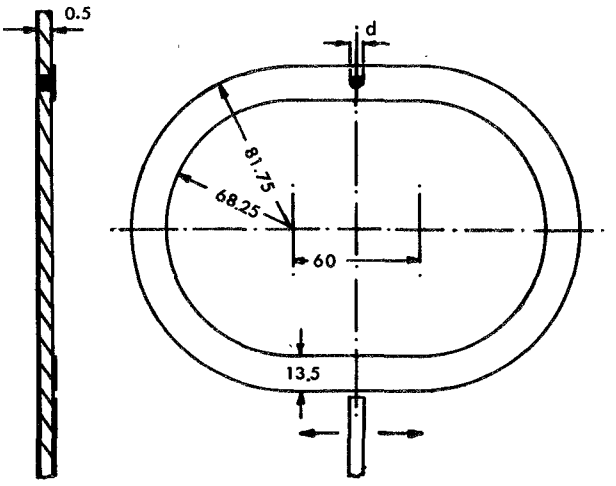

Fig. 6. Microstrip ring used for measuring the Z parameters of centered metallic posts (dimensions in centimeters).

In most cases, it will be necessary to stabilize the temperature of the substrate within ± 0.5°C if meaningful measurements are to be made.

Q factors are best measured in the transmission mode [5] which, unfortunately, requires a second coupling link between ring and peripheral equipment, but may be evaluated from reflection measurements with lesser accuracy. Fig. 5 shows the arrangement used for measuring the resonance frequencies of the microstrip ring.

IV. MEASUREMENT ACCURACY

The accuracy of the measurements is affected by the following sources of error:

1) mechanical and electrical imperfections of the ring;
2) temperature fluctuations;
3) uncertainty in the frequency measurements made on the empty ring (uncertainty in ϵ_{eff} and Q_1);
4) uncertainty in the frequency measurements made on the perturbed ring.

Items 1) and 2) can be minimized by constructing the ring with care and by placing it in a temperature-stabilized environment. Items 3) and 4) depend on the precision with which the resonance peaks and limits of the 3-dB bandwidth can be located. A good way to evaluate this precision is to locate the same resonance peak several times and find the standard deviation of the measured frequency values from the calculated average.

To obtain the sensitivity of Z_{ie} and Z_{io} of a lossless discontinuity to errors in frequency measurements, (9) and (10) are differentiated with respect to resonance frequencies. For both impedances, the result is

$$\frac{\Delta Z_i}{Z_i} = \frac{1 + |Z_i|^2}{jZ_i} \frac{\pi l_{\text{ring}} (\epsilon_{\text{eff}})^{1/2}}{c} (\Delta f_p - \Delta f_e) \tag{15}$$

where Δf_p and Δf_e are the absolute errors in the resonance frequencies of the perturbed and the empty ring, respectively. It can be seen that the relative error in Z_i depends on the value of Z_i itself. Z_i is least sensitive to measurement errors if its value is close to $\pm j1$. In the presence of losses, (15) applies to the imaginary parts of the discontinuity impedances only. Quality factors can be measured within 2–3 percent.

V. EXPERIMENTAL RESULTS

Measurements have been made on centered metallic posts of circular cross section in a ring which had the shape of a racetrack (Fig. 6). The discontinuity could thus be placed into a straight section of line, and the launcher could also be moved along a straight line on the opposite side. The ring had a characteristic impedance of about 27 Ω (W/h = 2.7) on a 5-mm Stycast substrate with a nominal dielectric constant of 10.6. Its mean circumference was $l_{\text{ring}} = 59.124$ cm.

The oversize substrate was chosen to minimize errors due to dimensional inaccuracies. The ring was placed into a temperature-controlled box and kept at 30.5 ± 0.4°C.

Cylindrical metallic posts were chosen because they could easily be introduced after measurements on the empty ring were made. The obstacles were realized by drilling a hole across the microstrip and filling it with mercury. This ensured good electrical contact at the strip and the ground plane, and the electrical parameters of the discontinuity could be reproduced within the limits of accuracy of the equipment.

Return loss measurements were performed in the range 0.1–2 GHz using a network analyzer. Frequencies were measured with a digital counter. Peaks of absorption could be localized within ±20 kHz.

The 3-dB linewidth of resonance ranged from about 0.7 MHz at low frequencies to about 2 MHz at high frequencies. The Q factor of the ring was so little affected by the discontinuities that they appeared to be almost lossless, and the accuracy in determining the resistances R and r was unsatisfactory. They are therefore not reported here.

Fig. 7 shows the dispersive effective dielectric constant obtained from the resonances of the empty ring. Figs. 8 and 9 present the

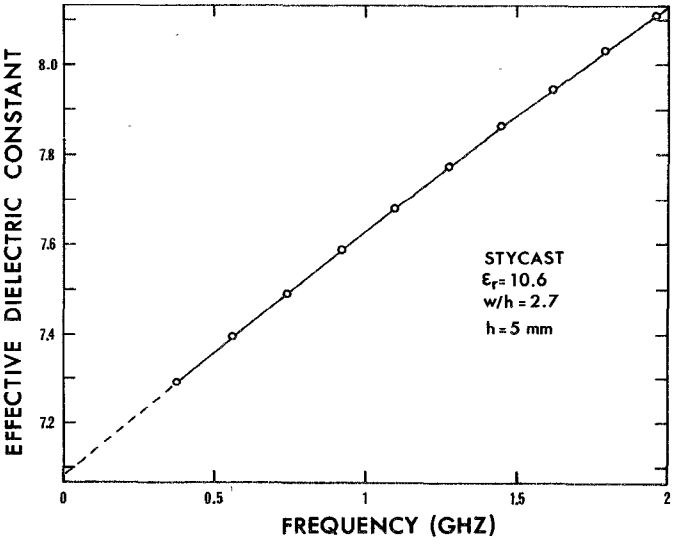

Fig. 7. Measured effective dielectric constant for the microstrip ring presented in Fig. 6.

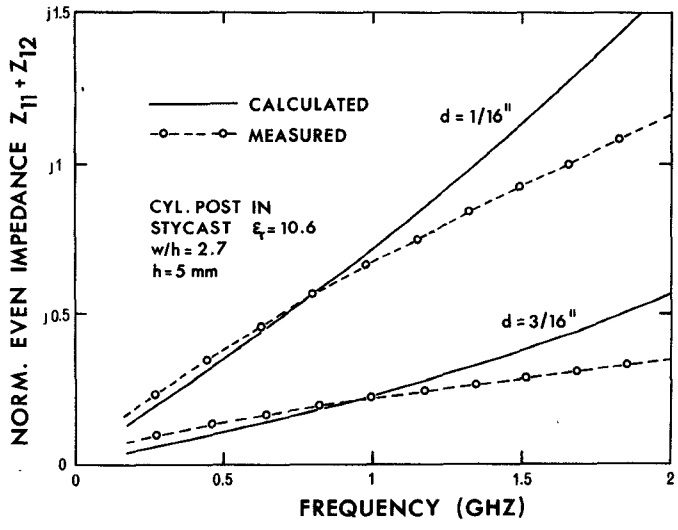

Fig. 8. Normalized even impedances of centered metallic posts of circular cross section in a 27-Ω line on Stycast (ϵ_r = 10.6; h = 5 mm; W/h = 2.7). Post diameter d = 1/16 in, post diameter d = 3/16 in.

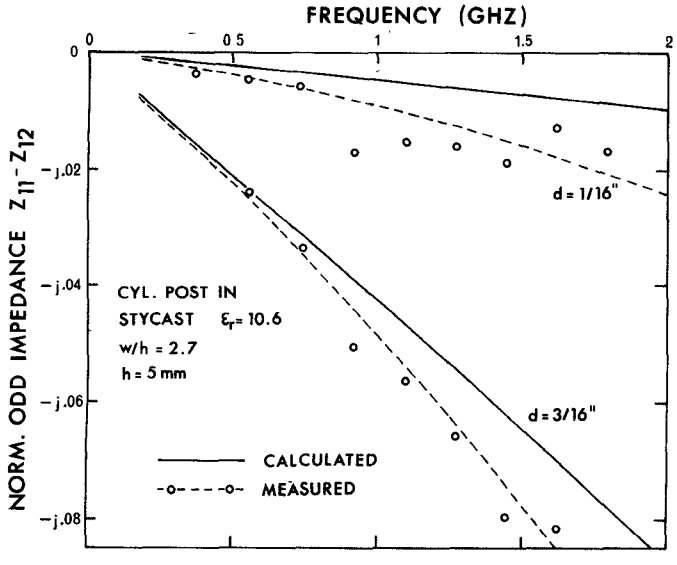

Fig. 9. Normalized odd impedances of centered metallic posts of circular cross section in a 27-Ω line on Stycast (ϵ_r = 10.6; h = 5 mm; W/h = 2.7). Post diameter d = 1/16 in, post diameter d = 3/16 in.

measured and calculated reactive impedances of posts of diameter $\frac{1}{16}$ and $\frac{3}{16}$ in for even and odd excitation.

It can be seen that the measured values for the even impedances form a smooth curve while the values measured for the odd impedance are more scattered. This confirms the observation made with respect to (15): the more the impedances differ from $\pm j1$, the more sensitive they are to errors in frequency measurements.

Taking into account the residual changes in temperature, small imperfections in the ring, and the uncertainties in the localization of resonance peaks, the total uncertainty in both f_p and f_e [in (15)] was typically ±50 kHz over the whole frequency range covered in the experiment. On this basis, the relative error in the discontinuity impedances is as shown in Table I.

The theoretical values which are presented in Figs. 8 and 9 for comparison are only approximate and differ from experimental results for the following two reasons.

1) They have been calculated using the variational principle and assuming only approximate simple current-distribution functions on the obstacle. If the correct current distribution were known, theoretical results would be closer to experimental values.

2) In these calculations, the microstrip was replaced by an idealized parallel plate model with magnetic sidewalls. This model does not incorporate radiation effects. Even though radiation losses appear to be very small, the reactive part of the radiation impedance affects the energy stored at the discontinuity. This phenomenon is currently being studied by the authors.

TABLE I
RELATIVE ERROR IN IMPEDANCE MEASUREMENTS AS A FUNCTION OF THE IMPEDANCE VALUE

$\lvert Z_i \rvert$	1	0.1	0.01	0.001
$\lvert \Delta Z_i/Z_i \rvert$	0.3%	1.8%	18%	180%

VI. CONCLUSION

The evaluation of the equivalent circuit of microstrip discontinuities in a resonant ring avoids the problems encountered when measuring through coaxial-to-microstrip transitions, the characteristics of which are poorly known. The Z parameters of a discontinuity are calculated from the resonant frequencies and Q factors of the ring before and after the introduction of the discontinuity. Normalized reactances between $\pm j100$ and $\pm j0.01$ can be measured with satisfactory accuracy. Evaluation of losses is more difficult since this involves measurement of changes in Q factors, a procedure which is inherently less accurate than the measurement of resonance frequencies.

The method is excellent for checking theoretical expressions for microstrip discontinuity parameters, and for characterizing microwave-integrated-circuit elements.

ACKNOWLEDGMENT

The authors wish to thank Dr. D. S. James for fruitful discussions and for supplying the microstrip ring.

REFERENCES

[1] I. M. Stephenson and B. Easter, "Resonant techniques for establishing the equivalent circuits of small discontinuities in microstrip," *Electron. Lett.*, vol. 7, pp. 582–584, 1971.
[2] R. J. P. Douville and D. S. James, "Experimental characterization of microstrip bends and their frequency dependent behaviour," presented at the IEEE Int. Electrical, Electronics Conf. Expo., Toronto, Ont., Canada, 1973.
[3] H. Groll and W. Weidmann, "Measurement of equivalent circuit elements of microstrip discontinuities by a resonant method," *Nachrichtentech. Z.*, vol. 28, pp. 74–77, Jan. 1975.
[4] N. Marcuvitz, *Waveguide Handbook*. Boston, Mass.: Boston Tech., 1964.
[5] W. J. R. Hoefer and G. R. Painchaud, "Frequency markers providing resolution of 1 kHz for swept microwave measurements," *Electron. Lett.*, vol. 10, pp. 123–124, Apr. 1974.

The Accurate Measurement of Range by the Use of Microwave Delay Line Techniques

GERALD F. ROSS, FELLOW, IEEE

***Abstract*—A scheme is presented for accurately measuring range to a radar target by the use of microwave delay line techniques and the use of solid-state subnanosecond digital threshold circuitry. The scheme obviates the need for expensive high-speed counters or analog thresholding and is cost effective to implement. A breadboard**

Manuscript received April 18, 1975; revised July 14, 1975, and August 27, 1975.

The author is with the Sensor Systems Department, Sperry Research Center, Sudbury, Mass. 01776.